Membrane materials targeting carbon capture and utilization

Guining Chen, Tianlei Wang, Guangru Zhang, Gongping Liu, Wanqin Jin [*]

State Key Laboratory of Materials-Oriented Chemical Engineering, College of Chemical Engineering, Nanjing Tech University, 30 Puzhu Road (S), Nanjing, 211816, China

ARTICLE INFO

ABSTRACT

Over the past decades, fossil fuel combustion has emitted large quantities of CO_2 into the atmosphere, resulting in global climate change. Nowadays, it's considered a feasible strategy to capture CO_2 from some significant point sources. Three main strategies have been developed, namely post-combustion, pre-combustion, and oxy-fuel combustion. Recent research indicates that the membrane technology for CO_2 capture has become competitive compared with conventional technologies because of the improved separation performance in materials and process designs. This paper mainly reviews the progress and breakthroughs of membrane materials for the three gas separation systems corresponding to the CO_2 capture strategies. Besides, the CO_2 utilization by the membrane process has also been highlighted.

1. Introduction

The climate environment has been dramatically affected because of the rapid development of industry and the dependence on fossil fuels. According to the latest CO_2 emission data supported by the global monitoring laboratory, the current concentration of CO_2 sits at ~416 ppm, which is excessively higher than what it was at the beginning of the last century [1]. This phenomenon has attracted serious concern in government organizations in the past few decades. The Intergovernmental Panel on Climate Change (IPCC) reports that human activities will cause a temperature increase of 1.5°C by 2030–2052 [2]. Consequently, United Nations Framework Convention on Climate Change (UN-FCCC) treaty was reached in the United Nation's Earth held in 1992 to control the concentration of CO_2 and other greenhouse gases in the atmosphere, which accelerated the research and development of CO_2 capture technologies.

Among various CO_2 emission sources, the power generation sector is considered to be a significant anthropogenic source. Therefore, the CO_2 capture technology from power plants has aroused great interest for many governments and researchers. At present, three main strategies are summarized for mitigation of CO_2 emission [3–6]: 1. The post-combustion process (CO_2/N_2): the CO_2 is separated from the low-pressure exhaust gas of fuel combustion in the air. 2. The pre-combustion process: the CO_2 is captured from syngas produced by gasification. 3. The oxy-fuel combustion: the fuel combustion is realized in a pure oxygen atmosphere, leading to mixed gases that mainly contain CO_2 and H_2O. Although the oxy-fuel combustion process does not involve the direct CO_2 separation, the exhaust gas with high CO_2 concentration will greatly facilitate the subsequent CO_2 separation and improve the capture efficiency. The general outline of the CO_2 capture process is illustrated in Fig. 1. In addition, natural gas purification and biogas sweetening (mainly involving CO_2/CH_4) will not be involved in this review, although membrane separation has achieved remarkable progress in this area.

Nowadays, the difficulty of CO_2 capture is to reduce energy consumption and capital cost. As of 2020, most commercial-scale carbon capture projects are in early development [7]. In numerous processes studied for CO_2 capture, membrane technology is known for its ease of installation, energy efficiency, flexibility in operation and maintenance, and the ability to overcome thermodynamic limitations [8]. It also requires very few chemicals compared to conventional separation processes. With the massive emission of CO_2, the demand for CO_2 capture provides an opportunity for the deployment and application of membrane materials.

This paper mainly reviews the materials selection and development for diverse scenarios. According to the three main carbon capture strategies, we reviewed popular materials including polymers, inorganics and hybrid materials and their separation performance, respectively. Subsequently, CO_2 utilization by membrane reactor was briefly discussed using some cases. Finally, we discussed the challenges and opportunities of membrane materials for CO_2 capture and utilization.
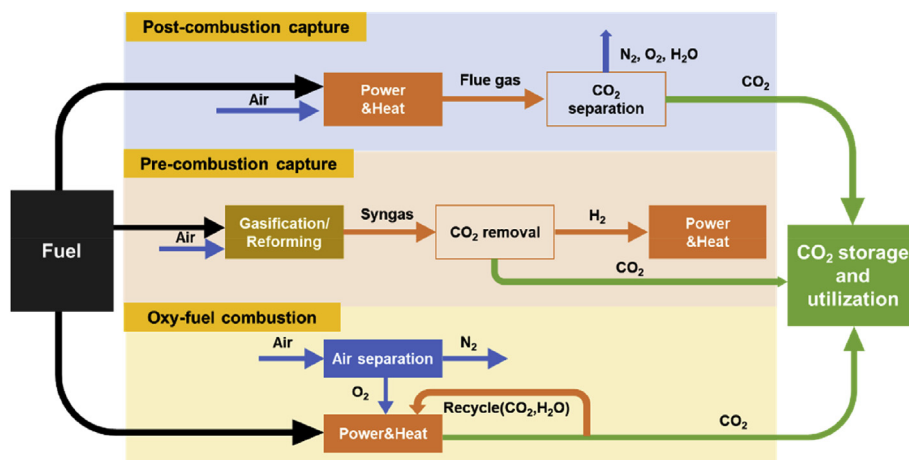
Fig. 1. Three CO_2 capture approaches from power plants.

2. Post-combustion

Post-combustion means the separation of CO_2 from flue gases produced by burning fossil fuels. Generally, flue gases are mainly composed of N_2, water vapor, and CO_2. The content of CO_2 is primarily controlled by the used combustibles. Due to the low CO_2 partial pressure and the enormous amount of flue gas, high CO_2 permeable membranes with moderate CO_2/gas selectivity are critical for the practical application of membrane technology in CO_2 capture.

2.1. Polymeric membranes

Among numerous membrane materials, polymer-based materials show intrinsic advantages in cost, processability, and variety. Generally, solution-diffusion and facilitated transport mechanism has been widely recognized and adopted to guide the design of new polymers. Polymers including polyacetylene, polyaniline, polyetherimides, polycarbonates, poly(phenylene oxide), poly(ethylene oxide), and polysulfone have been investigated for post-combustion. By manipulating polymer preparation and chemical composition, these membranes have highly tunable membrane permeability and selectivity. However, the swelling and plasticization caused by CO_2 adsorption cannot be neglected.

Among the efforts to enhance CO_2 performance, polymer blends and copolymers have shown high potential. In 1982, Kawakami et al. reported a pioneering work by blending a plasticizer polyethylene glycol (PEG) in a low permeable cellulose nitrate [9]. It was observed that membrane performance improved significantly with increasing PEG percentage and molecular weight. Subsequently, composite polymeric membranes with various groups or free volumes were developed for CO_2 separation to compensate for the defects of a single polymer or combine the advantages of multiple functional groups. Similarly, copolymers and cross-linked polymers have radiated greater vitality. One of the most famous copolymers is PEO-based materials.

Poly (ethylene oxide) (PEO) has been widely used to improve CO_2 permeability in membranes because of the high affinity towards CO_2 caused by the quadrupolar interactions of the polar ether group with CO_2 molecules. In 2012, Jiang group reported a new polyethylene oxide-*b*-polystyrene block copolymer which exhibited high CO_2 permeance over 20,000 Barrer [10]. The research demonstrated that the self-assembled microphase structures and functional block units played synergistic roles in the high membrane performance. In recent decades, a series of commercial membranes, e.g., Pebax®, Polaries®, and Polyactive® have been developed and proved to be promising candidates for post-combustion capture. The typical structure of Pebax® MH 1657 is shown in Fig. 2(a), where the amide groups (PA) account for 40%, and the ether linkages (PE) account for 60%. (1 Barrer $= 1 \times 10^{-10}$ cm^3(STP)
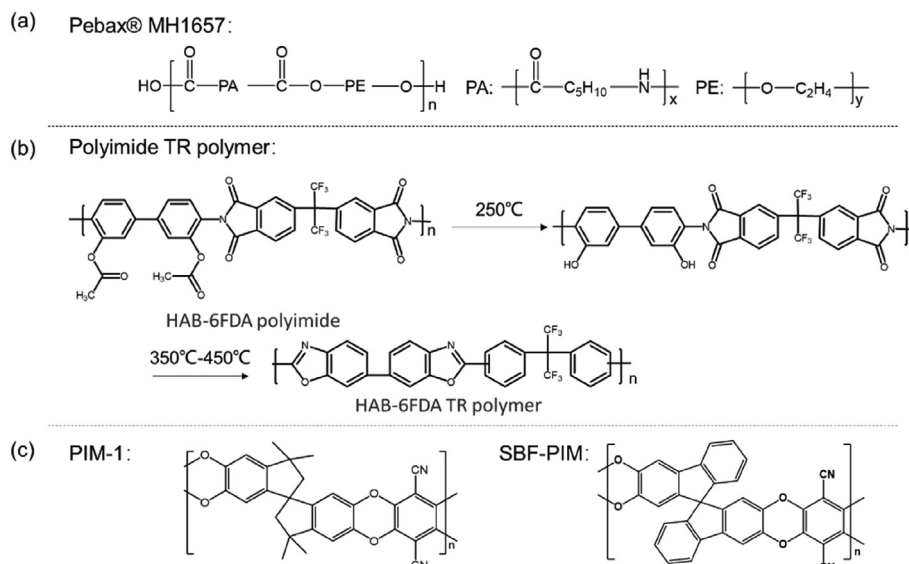

Fig. 2. (a) Pebax® MH 1657; (b) thermal rearrangement protocol of polyimide; (c) PIM-1 and PIM-SBF sturcture.

cm cm^{-2} s^{-1} cmHg^{-1} = 3.344 × 10^{-16} mol m m^{-2} Pa^{-1} s^{-1})

In 2007, Park and coworkers prepared new polymers via thermal rearrangement of polyimides and polyamides [11]. The thermal rearrangement process can generate high free volume and narrow cavities in polymers, resulting in a substantial increase in permeance by at least two orders of magnitude. Then, extensive works about the design of precursor structures and heat treatment protocols have been reported to optimize the separation performance and increase the mechanical strength. Freeman's group studied the influence of temperature in a polyimide precursor during thermal treatments [12]. Fig. 2(b) gives the reaction scheme where the polyimide HAB-6FDA was converted to polybenzoxazoles. The sorption coefficients of membranes showed the same upward trend with the increase in temperature. Sanders et al. compared a series of functional polyimide precursors and the resulting TR polymers [13]. Studies have shown that large functional groups can effectively inhibit the chain packing and increase free volume. Since the superior thermal stability and outstanding performance, TR polymers demonstrate bright application prospects in post-combustion.

Another well-known polymer with high permeability is polymers of intrinsic microporosity (PIM) reported by McKeown et al. in 2004 [14]. Due to the contortion of rigid polymer chains, PIMs have numerous interconnected pores smaller than 2 nm. The studies on PIMs are mainly focused on introducing rigid units and changing contortion angles to increase free volume to improve CO$_2$ permeability further. McKeown group reported a highly gas-permeable polymer using spirobifluorene as the central structural unit [15] (Fig. 2(c)). Subsequently, a series of PIMs prepared by Tröger's base were reported with membrane performance approaching 2008 upper bound [16].

Polymeric membranes mentioned above all belong to solution-diffusion transport-based membranes. Facilitated transport membranes with reactive carriers are another kind of high CO$_2$ permeable membranes where CO$_2$ transport is enhanced by interaction with CO$_2$ molecules through reversible reactions. Liquid membrane, ion-exchange membrane, and fixed carrier membrane are three primary forms of facilitated transport membranes. The advantages and disadvantages are listed as follows(See Tables 1 and 2).

The fixed carrier membranes are widely favorable because of their excellent permeability, low cost, and simple fabrication process. As the name implies, the carriers in fixed carrier membranes are covalently bonded and cannot move, so the selectivity of this kind of membrane is not high. Groups, such as –NH$_2$, CO_3^{2-}, -COO$^-$, are the conventional choice of CO$_2$ carriers. One typical fixed carrier membrane material is polyvinyamine (PVAm) which contains a high density of amine groups. In 2013, Hägg group reported that the pH control could remarkably enhance the PVAm performance for CO$_2$ capture [17]. It was found that the membranes prepared by higher pH casting solution had more amine groups, resulting in faster CO$_2$ transport. The facilitated transport mechanism is shown in Fig. 3.

Since the number of effective carriers plays an important role in membrane performance, different methods have been developed to increase the carrier concentration. In 2013, Qiao et al. reported a PVAm-PIP/polysulfone (PS) composite membrane [18]. High PIP loading improved the concentration of carriers and effectively reduced the

crystallinity of PVAm, bringing improved CO$_2$ permeance of 6500 GPU. Recently, they successfully synthesized metal-induced ordered microporous polymers (MMPs) via PVAm, divalent metal ions, and organic linkers [19]. The prepared membranes demonstrated excellent structural stability under humid and dry feed conditions, showing auspicious CO$_2$ capture performance. Recently, Winston Ho group synthesized an ultra-high molecular weight PVAm by inverse emulsion polymerization, which demonstrated an improved transport performance due to the alleviation of penetration and a higher amine content in the membrane. The PVAm based membrane with 85 wt% piperazine glycinate (PG) loading achieved CO$_2$ permeance of 839 GPU and a CO$_2$/N$_2$ selectivity of 161 at a typical flue gas temperature of 57°C [20]. Furthermore, they have successfully realized the scale-up fabrication of PVAm/PG-containing membranes in a roll-to-roll manner using the thin-film coating (TFC) assembly (Fig. 4). A total of >2000 feet long and 14-in. wide membrane with a selective layer thickness of <200 nm was successfully fabricated which showed good agreement with lab-synthesized membranes in CO$_2$/N$_2$ separation [21]. (Gas permeance unit, 1 GPU = 1 × 10^{-6} cm^3(STP) cm^{-2} cmHg^{-1} = 0.344 × 10^{-10} mol m^{-2} s^{-1} Pa^{-1})

2.2. Non-polymeric membranes

Compared with the remarkable progress of numerous polymeric membrane materials, non-polymeric materials such as zeolite, metal-organic framework, carbon molecule sieve have also been in an emerging stage of vigorous development in CO$_2$ separation. Usually, those membranes show better stability than polymeric membranes and thus are the leading candidates for gas mixtures separation, especially under harsh operating conditions.

Zeolites are crystalline microporous aluminosilicate frameworks built of corner-sharing AlO$_4$ or SiO$_4$ tetrahedra, employed in numerous applications such as purification, adsorption, separation, catalysis. Zeolite membranes used for CO$_2$ capture can offer high selectivity because of their well-defined pore structures. Several zeolites such as Na–Y [22], SAPO-34 [23], and MFI [24] membranes have been investigated for post-combustion. Kusakabe and coworkers reported excellent results of Na–Y membrane with CO$_2$/N$_2$ separation factor of 100 at 303 K [22]. Recently, Zhou group prepared defect-free SAPO-34 membranes on tubular alumina substrates [25]. At 243 K, the CO$_2$ permeability reached about 4100 GPU with selectivity about 110 with a CO$_2$/N$_2$ volume ratio of 15/85. Currently, SAPO-34 membranes show excellent separation performance far beyond the polymeric upper bound and demonstrate potential applications in industrial post-combustion.

Porous metal-organic framework (MOF) materials are also prevalent for CO$_2$ separation. In 2016, a high selective IRMOF-1 membrane was reported with CO$_2$ permeance over 600 GPU and CO$_2$/N$_2$ selectivity of 410 with a CO$_2$ mole fraction of 0.874 [26]. Noticeably, the membrane was nonselective when the CO$_2$ mole fraction was smaller than 0.65. Jomekian et al. tried coating a PDMS layer on ZIF-8 film, and the membrane selectivity was successfully improved from 5.7 to 13.5 with a slight CO$_2$ permeance reduction from 1044 GPU to 925 GPU [27]. Some other examples of the best results reported on CO$_2$/N$_2$ separation using zeolites and MOF membranes are listed below.

A carbon molecular sieve (CMS) was prepared with rich and rigid gas permeation channels by pyrolysis of polymer precursors. Koros group has done pioneer works on the control of pyrolysis conditions to explore its relationship and membrane performance [34,35]. Generally, the higher pyrolysis temperature means higher gas permeability and lower selectivity. Besides, the structural properties of precursors may also significantly affect the microstructure of CMS membranes, resulting in different gas separation performances. For example, Hou and coworkers investigated several CMS membranes made of polyimides with varying parts of diamine [36]. In Fig. 5, the CMS membrane with turbostratic carbon was fabricated by pyrolysis of polyimide precursor. The PPD-PMDA with linear structure and low fraction of free volume (FFV) resulted in a dense carbon structure where molecular sieving dominated the gas separation.

Table 1
Summary of the advantages and disadvantages of three facilitating transfer membranes.

	Carriers work form	Advantages	Disadvantages
Liquid membrane	move freely	Excellent performance	Poor stability
Ion-exchange membrane	held by electrostatic forces	Favorable stability; high selectivity	Low permeability
Fixed carrier membrane	vibrate in a confined space	High permeability; cheap	Moderate selectivity

Table 2
Top-performing zeolite and MOF membranes in CO_2/N_2 separation.

Membrane	Temp.(K)	Feed pressure(kPa)	CO_2:N_2 in the feed	$\alpha(CO_2/N_2)$	CO_2 Permeance (GPU)	Ref
Na–Y	303	300	1:1	100	450	[22]
SAPO-34	243	100	1.5:8.5	170	4120	[25]
SAPO-34	295	241	1:1	32	3500	[28]
ZSM-58	298	300	1:1	44	864	[29]
SSZ-13	298	303	1:1	32	954	[30]
AlPO-18	298	303	1:1	45	1880	[31]
IRMOF-1	298	505	8.74: 1.26	410	614	[26]
ZnTCPP	308	100	1:1	33	2070	[32]
CAU-1	29.8	100	9:1	22.7	3995	[33]
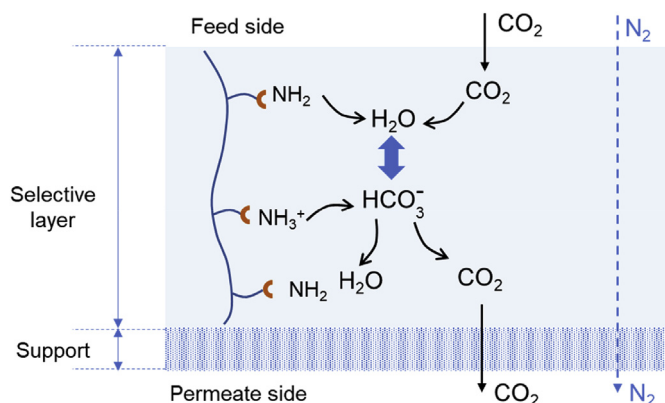
Fig. 3. Illustration of facilitated transport mechanism in PVAm membrane.

While carbon membrane prepared by BDAF-PMDA precursor with helical structure and high FFV showed looser structure accumulation, causing a CO_2 permeability about 3100 Barrer and moderate selectivity 21.8.

Except for the category materials mentioned above, some other inorganic materials have also performed well in CO_2/N_2 separation. In 2017, Yu group fabricated an ultrathin graphene oxide (GO)-based hollow fiber membrane using a facile coating process [37]. Under simulated flue gas conditions, it exhibited outstanding separation performance with a CO_2/N_2 selectivity as high as 680.

2.3. Mixed-matrix membranes

Mixed-matrix membranes (MMMs) formed by doping inorganic fillers into a polymer matrix received much attention due to the potential high separation performance and simple fabrication method. In 2013, Long group demonstrated that the CO_2 separation performance could be significantly enhanced by incorporating Mg_2(dobdc) nanocrystals within polyimide membrane [38]. Then, Xin et al. reported SPEEK based MMMs by incorporating PEI-decorated MIL-101(Cr) MOFs [39]. In Fig. 6(a), the

PEI was impregnated into MOF fillers via a facile vacuum-assisted method. Compared with MMMs doped unfilled MIL-101(Cr), the CO_2/N_2 selectivity of SPEEK/PEI@MIL-101(Cr) MMMs increased by 102.4%. Our group reported polyether block amide (PEBA) MMMs with UiO-66 NH_2 MOF fillers for CO_2 separation [40]. The amine-functionalized MOF particles showed a stronger affinity with CO_2 molecules and better dispersion in PEBA than unmodified MOFs. The MMMs with 10% UiO-66 NH_2 loading remarkably increased CO_2/N_2 selectivity from 43.2 to 72.2. Later, Yang group prepared MMMs with ionic liquid (IL)-modified ZIF-8 particles [41]. The confinement of ionic liquids in nanocages gave ZIF-8 filler an effective alteration of the molecular sieving properties for CO_2 separation. The IL@ZIF-8 MMMs demonstrated remarkable separation performance that transcend the upper bound of polymeric membranes.

In addition to porous MOF fillers, we reported a kind of MMMs by incorporating layered GO nanosheets for CO_2 capture (Fig. 6(b)) [42]. The GO nanosheets were assembled into regular GO laminates, showing proper channels for CO_2/N_2 separation. Amorphous polymer chains from TEM images surrounded the GO nanosheets, and the d-spacing of the two neighboring nanosheets was about 0.7 nm. This membrane exhibited preferential CO_2 permeability of 100 Barrer and excellent CO_2/N_2 selectivity of 91. Qiao and coworkers prepared a highly permeable aligned montmorillonite (AMT) MMM with a layered structure (Fig. 6(f)) [43]. It was found that the interlayer gaps of AMT were consistent with the orientation of the polymer chains and served as efficient CO_2 transport channels. From Fig. 6(g) and (h), the regular cuboid shape of MTs and highly orientated Na-exchanged MT were observed. This membrane exhibited CO_2 permeance of 800 GPU and good stability over 600 h. Overall, the variety of polymers and fillers such as zeolites, MOFs, MXene, etc., have extensively enriched the MMMs family for CO_2 capture, and some typical MMMs are summarized in Fig. 6(i).

3. Pre-combustion capture

Pre-combustion means removing CO_2 from the fuel before combustion. Pre-combustion is mainly used in the IGCC system, where H_2 and CO_2 can then be separated via a membrane separation system. In the case
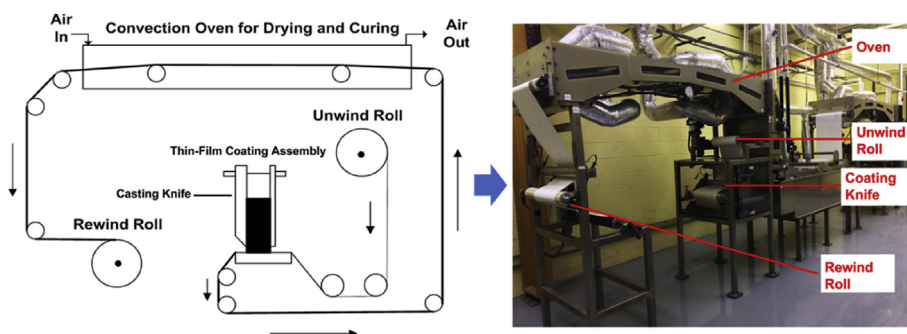
Fig. 4. Schematic and picture of the continuous pilot-scale machine with a TFC assembly for fabrication of thin-film composite membranes. Reprinted with permission from ref. 21. Copyright (2018) Elsevier.
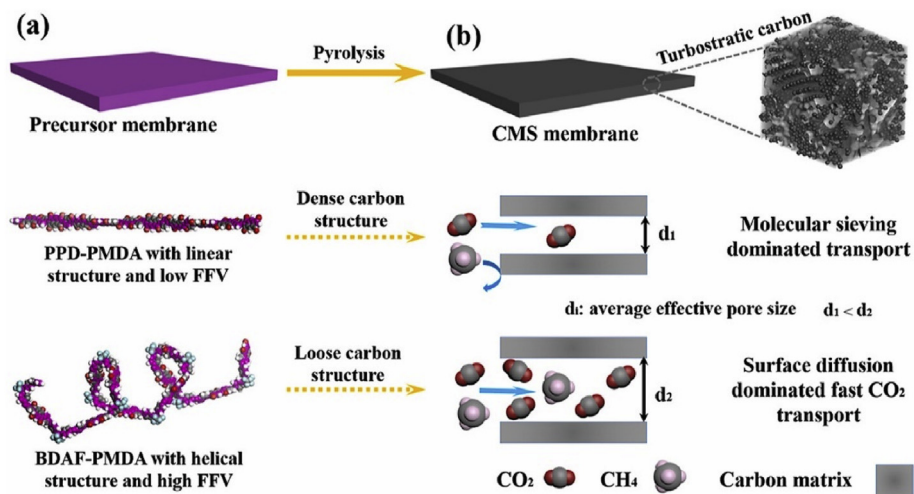
Fig. 5. Illustration of CMS membranes derived from different polyimide precursors. Reprinted with permission from ref.36. Copyright (2021) Elsevier.
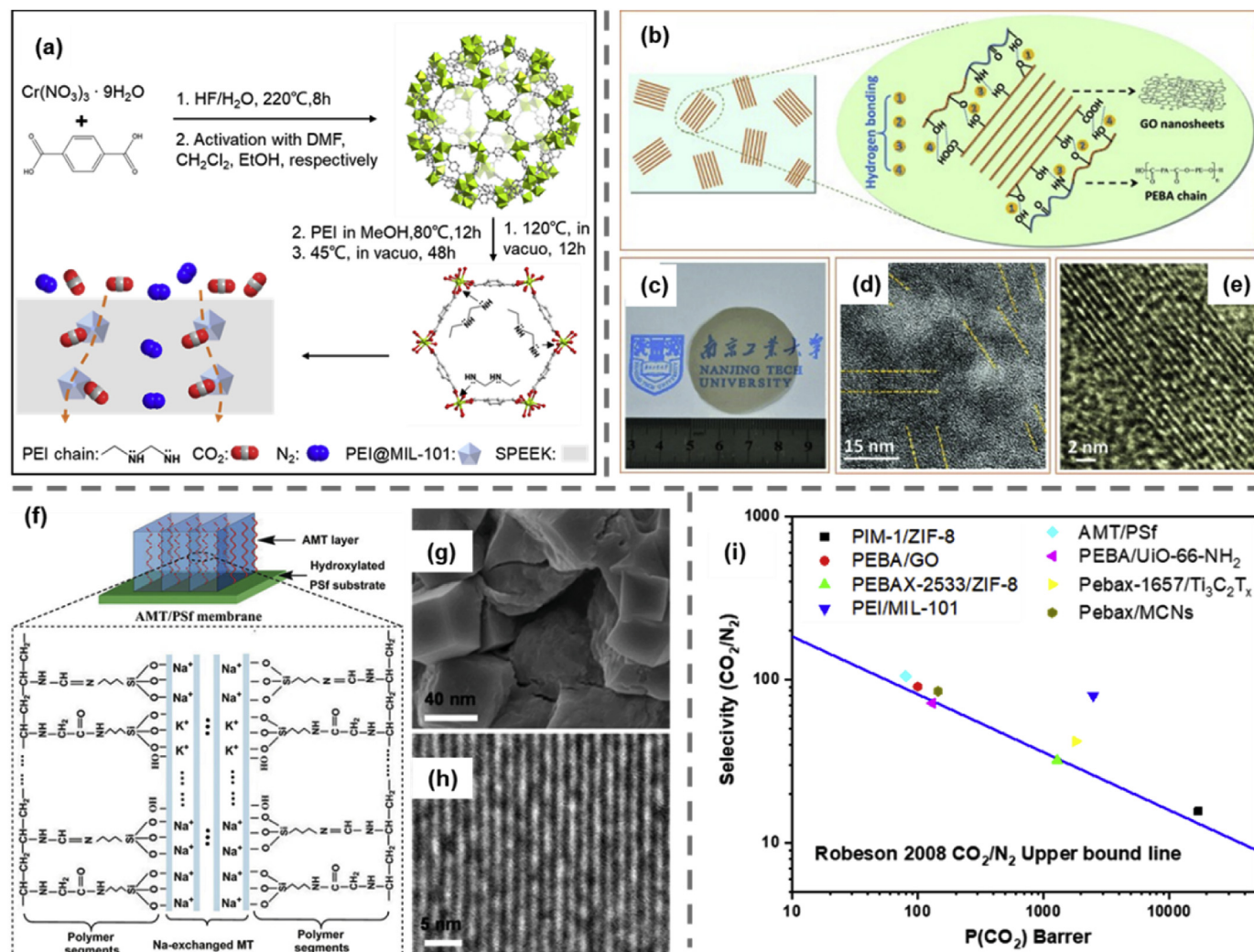

Fig. 6. (a) Illustration of the fabrication of PEI@MIL-101(Cr) based MMMs. (b)Schematic representation of GO/PEBA MMM, (c) digital photograph of free-standing GO/PEBA MMM, (d–e) TEM image of GO/PEBA MMM [42]. (f) AMT/PSf membrane, (g) surface SEM, and (h) AMT/PSf membrane TEM [43]. (i) Robeson 2008 CO_2/N_2 upper-bound line [44] and the separation properties of some typical MMMs including Pebax-based MMMs [39,41,45–47], PIM-1/ZIF-8 [48], AMT/PSf [44] and PEI/MIL-101 [39]. (b–e) Reproduced from ref. 42, copyright 2014 John Wiley & Sons. (f–h) Reproduced from ref. 43, copyright 2016 John Wiley & Sons.

of pre-combustion, the mixtures of CO_2 and H_2 are at high pressure and high temperature, which provide sufficient driving force for membrane separation. The IGCC process allows the application of two kinds of membranes: H_2-selective and CO_2-selective membranes. In this review, membranes that permeate H_2 are the focus since they are the most available.

3.1. H₂/CO₂ separation membranes

3.1.1. Non-polymeric membranes

Among H_2-selective membranes, metallic membranes are widely investigated because of the high H_2 purity up to 99.99% when using palladium (Pd) as the membrane materials [49]. For Pd-based membranes, the hydrogen separation process is realized by three steps: First, hydrogen is dissociated and chemically adsorbed on the surface to produce atomic hydrogen. Then, atomic hydrogen diffused to the opposite side of the Pd membrane through the metal lattice driven by the partial pressure drop. Finally, atomic hydrogen was recombined into H_2 molecules again, and the H_2 transmission was completed. The H_2 permeability rate is greatly affected by the membrane surface roughness, metal purity, and metallic lattice during this process. Besides, the Pd membrane exhibits improved performance at higher temperatures. Generally, ultra-thin metallic layers were coated on porous inorganic supports to obtain high H_2 flux and reduce costs. Ma group studied the Pd membrane performance with porous stainless substrates under different conditions

[50]. The membrane showed high H_2 permeance of 34 m^3/m^2 h $bar^{0.5}$ at $400°C$ under H_2/H_2O (10–37%) mixed gas conditions. Since the poor H_2 permeance of most Pd membranes, binary and complex alloys of Pd have been proven to be an effective method to improve H_2 permeability. Tong group reported a defect-free Pd–Ag membrane with submicron thickness. The membrane exhibited high separation fluxes of up to 4 mol of H_2/m^2·s at $450°C$ [51]. However, Pd-based membranes are vulnerable in many aspects, including hydrogen embrittlement, the presence of contaminants, limited lifespan, and high membrane costs. These drawbacks have primarily reduced their attractiveness in H_2 separation.

Except for metallic membranes, silica, zeolites, and MOFs have also been investigated for H_2/CO_2 separation. In 1998, Renate and coworkers reported a series of defect-free silica membranes [52]. Silica membrane calcined at $600°C$ showed H_2 permeance of 1474 GPU at $200°C$ and H_2/CO_2 selectivity about 71. However, researchers found that silica-based membranes were susceptible to humidity, and thus apparent performance decline was observed when exposed to high water vapor concentrations. This phenomenon was also observed in CMS membranes, where the water vapor blocks the membrane's pores, decreasing gas permeance. Surprisingly, the cellulose-derived CMS membrane showed excellent stability under high humidity due to its high hydrophilicity [53]. Lei and coworkers recently reported cellulose-based carbon hollow fiber membranes (CHFMs) with ultra-microporous of 3–4 Å for superior H_2 separation [54]. The prepared carbon membranes exhibited apparent asymmetric structural morphology (Fig. 7(a and b)). From Fig. 7(c), an
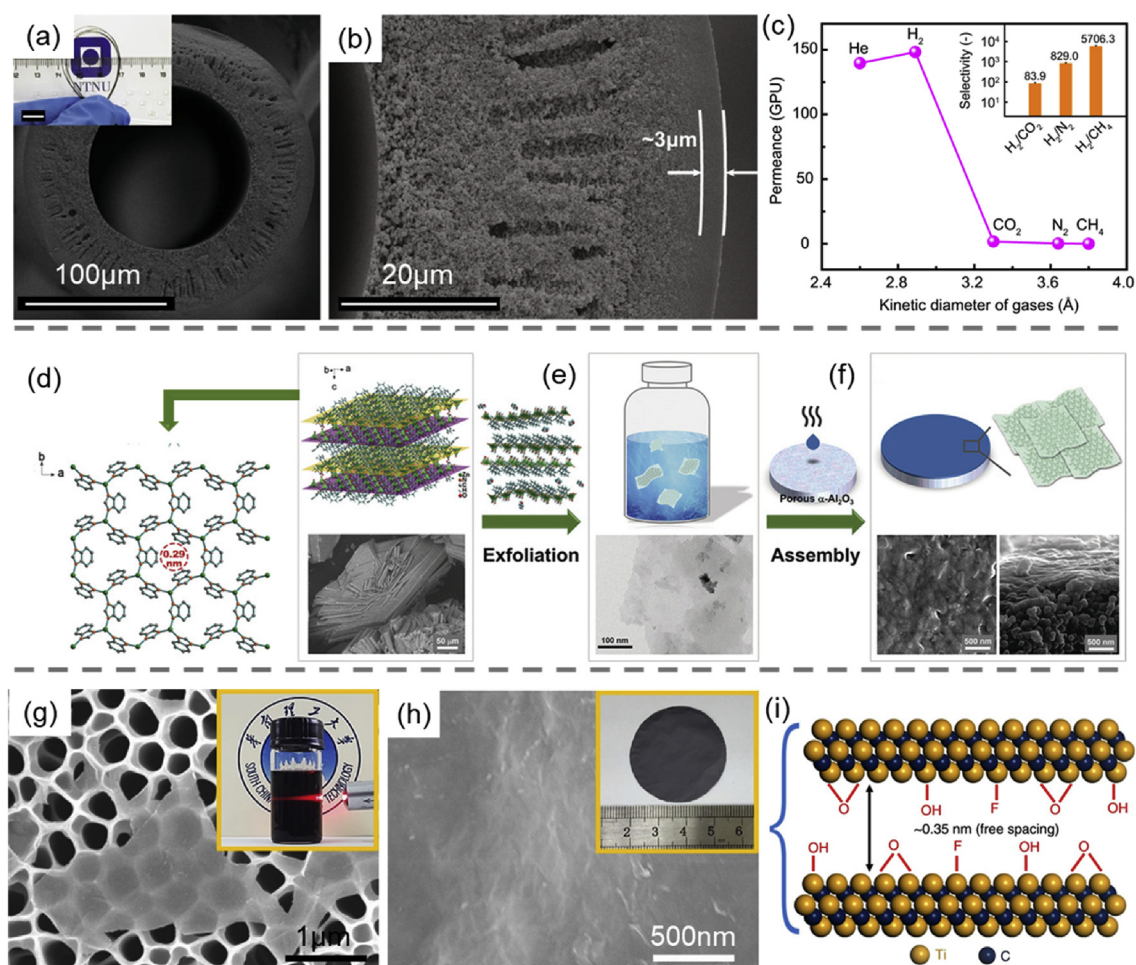

Fig. 7. (a–b) Cross-sectional SEM images of CHFM-700. (c) Single-gas permeances of CHFM-850 membrane at $130°C$ and 2 bar. (d–f) Schematic diagram of the $Zn_2(bim)_3$ membrane fabrication processes. (g–h) SEM pictures of delaminated MXene nanosheets and membrane surface. (i) Illustration of two adjacent Mxene nanosheets. (a–c) Reproduced from ref. 54. Copyright 2021 Nature Publishing Group. (d–f) Reproduced from ref. 59, copyright 2017 John Wiley & Sons. (g–i) Reproduced from ref. 61. Copyright 2021 Nature Publishing Group.

explicit cutoff between H_2 and CO_2 was observed. The membrane exhibited not only high separation performance but also good water vapor stability.

Unlike silica and CMS membranes, where microporous structures mainly depend on the calcination or pyrolysis step, the porous properties of zeolites and MOFs depend on the connection methods. So far, many zeolites and MOFs materials have been reported, which dramatically expands the candidates for H_2/CO_2 separation. For example, Dong and coworkers reported an on-stream modified MFI zeolite membrane. The membrane obtained H_2 single gas permeance of 555 GPU with H_2/CO_2 selectivity of 17.5 [55]. Caro group fabricated a ZIF-95 membrane which displayed H_2 permeances of about 5700 GPU and H_2/CO_2 selectivity of about 25.7 [56]. Later, Huang et al. used ZIF-95 nanosheets as seeds for ZIF-95 membrane preparation [57]. Although the membrane showed an evident decline in H_2 permeance (~500 GPU), the selectivity was improved to 41.6. In 2014, Yang group adopted $Zn(bim)_2$ nanosheets as building units to prepare molecular sieving membranes [58]. The prepared membrane achieved H_2 permeance of about 3000 GPU, and selectivity greater than 200, far beyond 2008 polymeric upper bound. Later, they developed a similar $Zn_2(bim)_3$ membrane with a static honeycomb-like aperture of 0.29 nm [59]. The detailed membrane fabrication processes were represented in Fig. 7(d–f). The prepared ultrathin membranes showed a remarkable separation performance owing to the size-exclusion effect of $Zn_2(bim)_3$ structure.

Besides MOF nanosheets, other 2D materials, including GO and MXene have been reported for H_2/CO_2 separation. In 2016, Our group reported the manipulation of GO-assembled 2D channels by external forces [60]. The prepared membrane with an interlayer height of about 0.4 nm demonstrated higher H_2 permeance and enhanced H_2/CO_2 selectivity. In 2018, Wang group reported lamellar MXene membranes with ordered nanochannels [61]. The membrane exhibited excellent H_2 permeability of more than 2200 Barrer and H_2/CO_2 selectivity over 160, better than most advanced membranes. From Fig. 7(g), the MXene nanosheets were very thin, and the Tyndall scattering effect was visible. The free spacing of the adjacent MXene nanosheets was about 0.35 nm (Fig. 7(i)), serving as an effective molecular sieve for H_2 and CO_2 gas mixtures.

3.1.2. Polymer-based membranes and mixed-matrix membranes

In terms of molecular kinetic sizes (H_2: 0.289 Å, CO_2: 0.33 Å), the diffusivity of H_2 is greater than that of CO_2. However, most polymers show affinity with CO_2, leading to the solubility of H_2 over CO_2 smaller than one. Generally, polymeric membranes with H_2 preferential permeation mainly depend on diffusion selectivity while the CO_2 solubility is inhibited. Because of size-sieving ability, a wide range of glassy polymers such as polysulfone (PSf) and polyimide have shown H_2/CO_2 separation performance. However, they suffer from low permeability (10–50 Barrer) and/or low H_2/CO_2 selectivity (1–10) and the trade-off restriction between permeability and selectivity. MMMs based on PSf and polyimide have been considered an effective way to achieve a breakthrough in permeance. For example, Leo group incorporated palladium (Pd) nanoparticles into PSf matrix where Pd nanoparticles were stabilized using polyvinylpyrrolidone (PVP). The MMM with 2% Pd loading exhibited high H_2 permeability of 5779 Barrer and satisfactory H_2/CO_2 selectivity of 6.2 [62]. Musselman and coworkers reported (Al) NH_2-MIL-53/V-TEC™ polyimide (PI)-1388 MMMs H_2/CO_2 mixture separations at high pressure and high temperature. At 300°C, the MMMs demonstrated simultaneous enhancement in permeability and selectivity (H_2 permeability: 85 Barrer to 144 Barrer, H_2/CO_2 selectivity: from 4.0 to 5.8) [63].

Polybenzimidazole (PBI) is another promising candidate among those polymer materials due to its high H_2/CO_2 selectivity, superior thermal and moisture stability, and excellent chemical resistance. However, the PBI membrane exhibits low H_2 permeability resulting from dense polymer chain packing. Therefore, strategies to improve H_2 permeability while simultaneously keeping selectivity are required to make it more industrially attractive. It was found that modification of main chain

structure could disrupt PBI chain packing and improve H_2 permeability (up to 997.2 Barrer), which was much higher than commercially available poly(2,20-(m-phenylene)-5,50-bibenz-imidazole) (m-PBI) (76.81 Barrer) [64]. However, lower H_2/CO_2 selectivity of about 5–7 was also observed versus m-PBI membrane of 23. Yang and coworkers prepared ZIF-8/PBI MMMs with higher solubility and diffusion coefficients [65]. The ZIF-8/PBI membrane with 30 wt% loadings had H_2 permeability of 470.5 Barrer with an H_2/CO_2 separation factor of 26.3. Recently, Lin group demonstrated a new kind of PBI membranes doped with polyprotic acids, which showed unprecedented size-sieving ability in H_2/CO_2 separation [66]. In Fig. 8(a), the cross-linking of PBI chains was achieved by transferring protons from H_3PO_4 to imidazole rings of PBI. A series of H_3PO_4 doped PBIs were prepared by immersing PBI membranes in solutions containing H_3PO_4 and methanol. When the molar ratio of PBI and H_3PO_4 was 1:1, the membrane exhibited an H_2/CO_2 separation factor of 140, far beyond the previously known polymeric materials [67].

TR polymers and PIMs have also been widely investigated for precombustion. For example, Lee and coworkers prepared different TR poly(benzoxazole-co-amide) membranes derived from monomers [68]. Among those membranes, the best performing membrane exhibited an H_2 permeability of 26.8 Barrer and H_2/CO_2 separation factor of 8.0 at 210°C. Later, a series of Tröger's Base based copolyimides were synthesized [69]. Although high H_2 permeabilities (249–667 Barrer) were observed, they all suffered from low H_2/CO_2 selectivity (highest: 2.8).

In 2018, Gascon group reported a facile interfacial polymerization to prepare supported benzimidazole-linked polymer membranes (Fig. 8(b)) [70]. A brown layer was quickly observed at the liquid interface due to the reaction of amine groups with aldehyde moieties (Fig. 8(d)). The growing film served as a barrier and confined the reaction to defective areas, guiding the formation of a dense and defect-free membrane.

3.2. CO₂/H₂ separation membranes

When H_2 production is of high priority, the CO_2-selective membrane is more favorable because it reduces H_2 loss during the separation process and helps to reach almost 100% CO conversion in an equilibrium-dominated low-temperature water-gas shift reactor. For polymer membranes with CO_2 selectivity, it is essential that the membrane strongly favors CO_2 and minimizes H_2 diffusion. Some polymeric membranes mentioned in CO_2/N_2 separation can also be used in CO_2/H_2 separation. For example, Freeman group investigated the mixed gas permeation of syngas components in PDMS and PTMSP. The CO_2 permeability and CO_2/H_2 selectivity of the PDMS membrane are 3200 Barrer and 3.4, respectively [71]. Bondar and coworkers demonstrated that the PEBA membrane showed higher CO_2/H_2 selectivity when polar group concentration was increased [72]. These high selectivity values may attribute to the large solubility selectivity in favor of CO_2.

As an extension of polymeric membranes, facilitated transport membranes usually demonstrate high CO_2 permeability and excellent CO_2/H_2 selectivity greater than 100 due to the complexation reaction between CO_2 and facilitator. Generally, amino species, polar groups and ionic liquids are popular choices. Winston Ho group has done much work on facilitated transport mechanisms containing amino species. They induced amines in crosslinked poly(vinyl alcohol) and the CO_2 permeability and CO_2/H_2 selectivity of the membrane at 120°C reached 8200 Barrer and 450, respectively [73]. Recently, they reported amine-containing MMMs incorporating amino-functionalized multi-walled carbon nanotubes (AF-MWNTs) for CO_2/H_2 separation. The MMM showed a selectivity of 205 and a CO_2 permeability of 3196 Barrer at 107°C and 0.2 MPa. However, reduced transport performance was observed due to the carrier saturation [74].

4. Oxy-fuel combustion

Oxy-fuel combustion is burning hydrocarbon fuel in an environment close to pure oxygen instead of air. It can generate flue gas containing
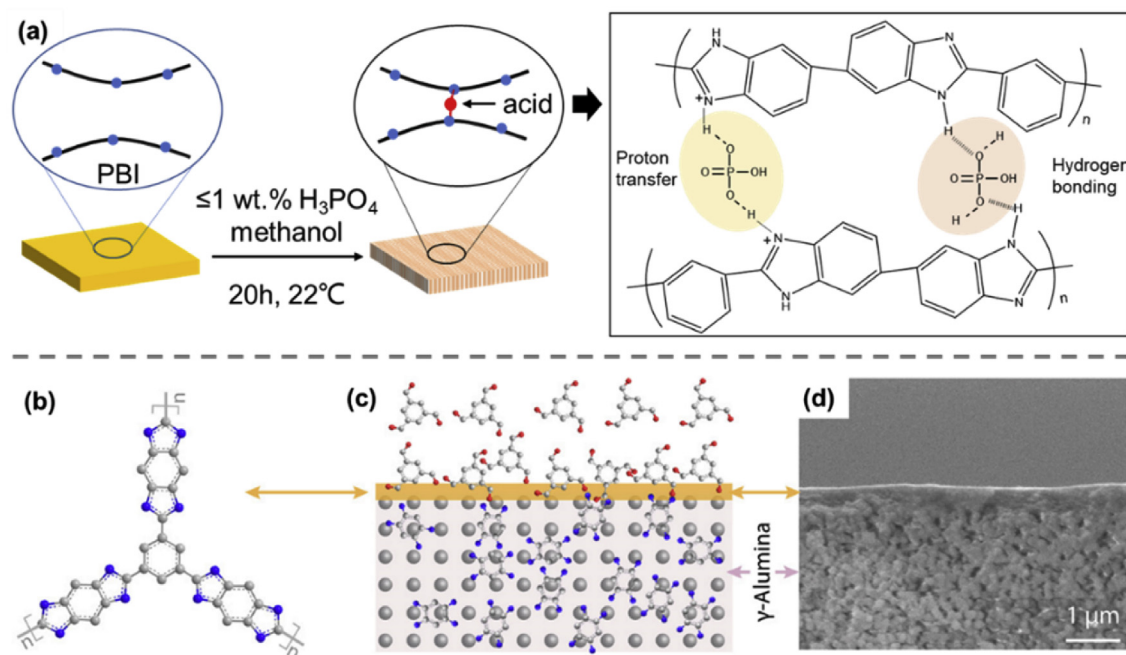
Fig. 8. (a) Schematic illustration of PBI membrane doped H_3PO_4. (b–d) Scheme of the formation of BILP-101x membrane. (b–d) Reproduced from ref. 70, copyright 2018 American Chemical Society.

very high CO_2 and water vapor concentrations, facilitating the post-combustion process. Besides, this process can significantly reduce burnout time and NO_x emissions, and exhaust gas volumes. Currently, various membranes have been studied for O_2/N_2 separation.

4.1. Polymer-based membranes and mixed-matrix membranes

For polymeric membranes, the solution-diffusion mechanism is dominant in O_2/N_2 separation [75]. Polysulfone (PSf), polyamide (PA), polyurethane (PU), polydimethylsiloxane (PDMS) and polyimide (PI) have been studied for O_2 preferential permeation. Among them, PSf has great potential because of its good mechanical strength and balanced permeability and selectivity. In 2002, Wang and coworkers reported PSf hollow fiber membranes with a dilute silicone coating layer [76]. The prepared membrane exhibited O_2 permeance of 20–30 GPU and O_2/N_2 selectivity of 5–6.5 at 25°C. Another popular O_2/N_2 separation material is polyimide. Koros and coworkers reported a kind of 6FDA-IPDA PI hollow fiber membrane, which led O_2 permeance of 65 GPU and O_2/N_2 selectivity of 6.3 [77]. Later, Kawakami group reported asymmetric 6FDA-FAP PI membrane with higher O_2 permeance of 794 GPU and low O_2/N_2 selectivity of 5.3 [78]. As to microporous polymers, although PIM-1 shows high O_2 permeability, the poor O_2/N_2 selectivity hinders its practical application [79].

In 2011, Zornoza and coworkers prepared PSf-based MMMs combining MOFs and zeolites fillers. The results indicated that the combination of HKUST-11 and silicalite-1 produced significant O_2/N_2 selectivity achievements and ZIF-8-PSf MMM exhibits the best O_2 permeability and O_2/N_2 selectivity which are increased by 63% and 80%, respectively [80]. Zhang group reported a composite membrane with PIM and cobalt IL $Bmim_2Co(NCS)_4$ [81]. When the loading of $Bmim_2Co(NCS)_4$ exceeded 0.4 wt%, the membrane exhibited O_2/N_2 separation performance beyond the 2008 Robeson upper bound.

4.2. Microporous inorganic membranes

Since the kinetic diameters of O_2 (3.46 Å) and N_2 (3.64 Å) molecules are very close, selectivity supported by Knudsen-diffusion can be ignored in microporous membranes. Similar kinetic diameters also bring

difficulties for inorganic membranes based on molecular sieving. Compared to the mediocre performance of zeolites and MOFs, CMS membrane performs quite well [82]. For example, Koros group investigated 6FDA/DETDA:DABA(3:2) derived CMS membranes with different pyrolysis temperature [83]. The CMS membrane pyrolyzed at 800°C showed desirable O_2 permeability and selectivity of 683 Barrer and 8.0, respectively. Liu et al. doped ZSM-5 nanoparticles into a carbon matrix [84]. A prominent O_2 permeability increment from 2.21 to 431 Barrer and a slight O_2/N_2 rise from 13.8 to 14.4 was observed when ZSM-5 content was 9.1 wt%.

4.3. Mixed ionic-electronic conducting (MIEC) membrane

MIEC membrane is a good choice for pure oxygen separation. Unlike the membranes mentioned above, MIEC membrane is dense membranes with 100% theoretical selectivity to oxygen. In MIEC membrane, oxygen in the form of ions diffuses from one side to the other via oxygen vacancies in the lattice (Fig. 9(a)). Such a permeation process requires the membrane material to have both oxygen ion conductivity and electronic conductivity. Perovskite, with the generic composition $ABO_{3-\delta}$, is the most studied MIEC for oxygen permeable material. The partial substitution of A or B sites can generate oxygen vacancies which can induce the adsorption of oxygen and act as an oxygen carrier to migrate oxygen ions to the other side of the membrane surface (Fig. 9(b and c)) [85].

To improve O_2 flux, numerous new perovskite materials have been reported. The main strategies of developing new perovskite membrane materials are focused on the changes in the A or B metal elements and the variations in the stoichiometric coefficient of the composition. For example, Sr, Ba, and La at the A site and transition elements Fe, Cr, and Co at the B site have become the popular choice [86]. However, the application of perovskite membranes was hindered due to poor structure stability, oxygen flux, and high operating temperature. To overcome these shortcomings, much work has been done to design new perovskite materials. For example, our group found that ZrO_2 doped $SrCo_{0.4}Fe_{0.6}O_{3-\delta}$ with remarkable structural stability under CO_2 or H_2 containing atmospheres [87]. Yang et al. successfully synthesized a series of $BaCe_xFe_{1-x}O_{3-\delta}$ perovskite membranes. Under a reductive atmosphere, these membranes showed both high permeability and stability [88].
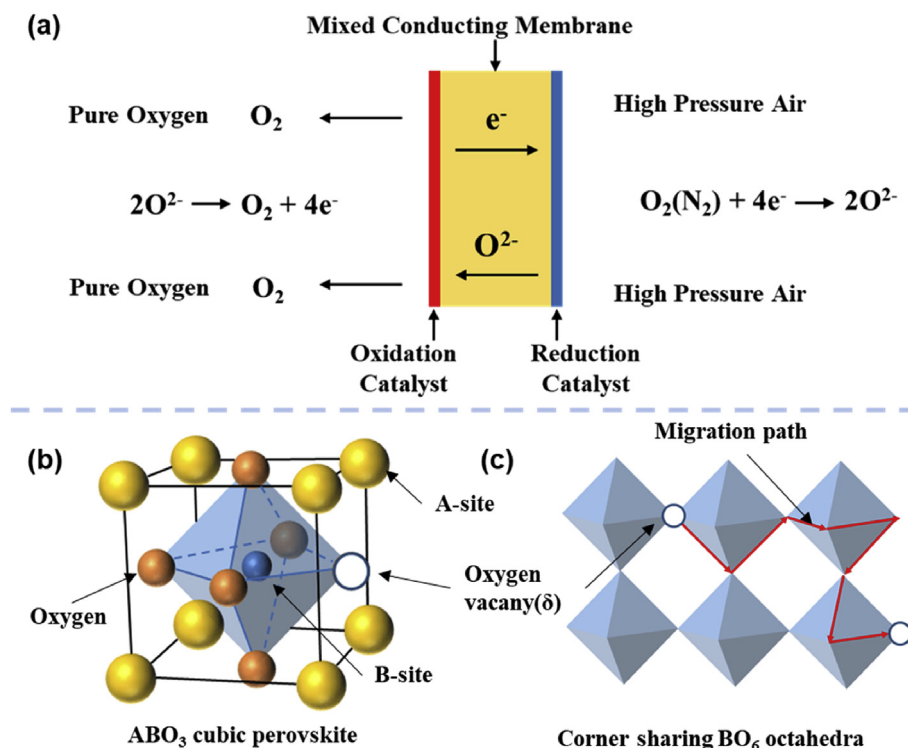
Fig. 9. (a) Mechanism of oxygen separation by MIEC membrane; (b) illustration of perovskite and (c) oxygen transport path.

Later, we reported unprecedented perovskite oxyfluoride membranes with F^- doping on O-site [89]. It was found that F^- could effectively weaken the chemical bonds of the perovskite structure, leading to enhanced oxygen permeability and reduced oxygen permeation activation energy. At low temperatures, the membrane exhibited extraordinary oxygen permeation performance, which completely fulfilled the commercial requirements.

In addition to the characteristics of the perovskite itself, the membrane configuration and preparation method, which determines the specific surface area and mechanical strength, also plays an important role in oxygen flux and structural stability. Researchers have designed many methods to prepare membranes, including multilayer structures with various architectures. Jin et al. first put forward the idea of synergistic shrinkage (i.e., the porous support and film shrink simultaneously in the sintering process) and developed a new method for preparing supported oxygen permeable membrane [90]. This idea was adopted and applied by the internationally famous company Air Products. Recently, our group developed a one-step thermal processing approach for efficient, high-performance perovskite hollow fibers production [91].

Compared with the traditional process, including mixing raw materials, two-step heating, repeated grinding, and phase inversion, the new approach was greatly simplified. Besides, multichannel hollow fiber membranes were designed and fabricated (Fig. 10(b)). Multichannel tubular membrane and hollow fiber membrane provided both high flux and high mechanical strength [92]. The 19-channel hollow fibers showed a mechanical strength of more than 50 N and could directly build an oxygen-permeable device or membrane reactor [93].

5. CO₂ utilization

As the main driver of climate change, CO_2 utilization technologies have recently received increasing attention. CO_2 utilization routes include enhancing oil and gas recovery, chemical conversion, mineralization, etc. Notably, converting CO_2 into fuels is considered the best way in CO_2 utilization. For example, Chen and coworkers reported an effective catalytic reverse water-gas shift (RWGS) process to produce CO with simultaneous CO_2 capture by a ceramic-carbonate dual-phase membrane reactor [94]. A CO_2 conversion of 56.8% and a CO production rate of
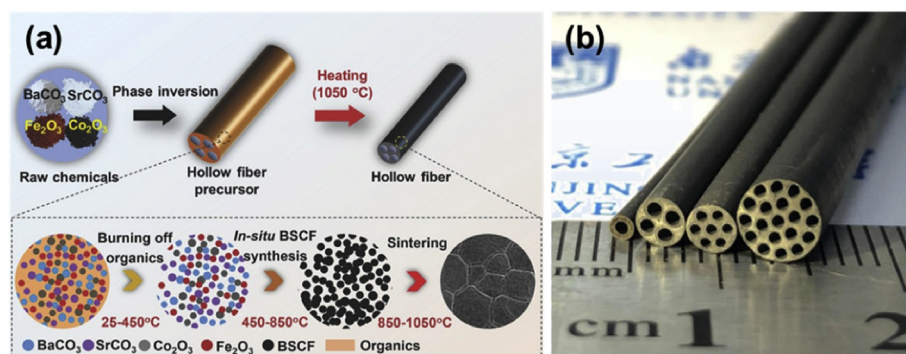

Fig. 10. (a) Schematic diagram of one-step thermal processing approach [91]. (b) Photo of multi-channel perovskite hollow fiber membranes. (a) Reproduced from ref. 91, copyright 2018 John Wiley & Sons.

2.41 ml min^{-1} cm^{-2} was obtained at 750% with La$_{0.9}$Ce$_{0.1}$NiO$_{3-\delta}$ catalyst. In addition to CO, methanol is another attractive product of CO_2 hydrogenation. Recently, Yu group reported NaA zeolite membrane with sodium ion (Na$^+$)-gated water-conduction nanochannels for CO_2 hydrogenation [95]. The in-situ water removal through the membrane continuously promoted the CO_2 conversion and methanol yield. Compared with a traditional reactor with copper-zinc-alumina catalysts (CO_2 conversion: 23.0%, methanol space-time yield (STY): 339 mg g$_{cat}^{-1}$hour^{-1}), the membrane reactor incorporating the water-conduction membrane greatly boosted CO_2 conversion and methanol STY to 61.4% and 809 mg g$_{cat}^{-1}$hour^{-1}, respectively. Followed by this work, huang group reported a similar bifunctional catalytic membrane reactor with different zeolite and catalytic [96]. The CO_2 conversion and methanol selectivity reached 36.1% and 100%, respectively.

A membrane reactor has also been applied in the thermal decomposition of CO_2. Here, our group proposed integrating the thermal decomposition of CO_2 with the partial oxidation of CH_4 (POM) using dense mixed-conducting membrane reactors [97]. Such a membrane reactor could in situ remove oxygen and promote the conversion rate of CO_2 to 11%, which was much higher than the original CO_2 conversion rate (0.00052%). Then, the lifespan of the membrane reactor was significantly extended by modifying the porous protective layer on the surface of the membrane [98]. We prepared a coupled reaction condition for a porous-dense-porous triple-layer composite membrane (Fig. 11) [99]. Due to the catalytic modification layer on the oxygen permeable side and the protective layer on the methane side, the CO_2 conversion rate reached 20.58%. It was operated stably for more than 500 h.

Generally, various industries have great potential to use CO_2 as a renewable resource rather than isolating it underground or in the oceans. Integrated systems like membrane reactors have provided good solutions for CO_2 utilization.

6. Summary and conclusions

In recent decades, people have shown increased interest in carbon capture and utilization. Some typical performance comparison was summarized in Fig. 12. As an alternative technology, membrane development has been in an emerging stage. In this article, the development of materials from post-combustion, pre-combustion, and oxy-fuel combustion is reviewed. Key achievements and challenges of membrane materials on each process are concluded as below:

(1) Post-combustion (CO_2/N_2): for polymeric materials including PEO-contained membranes, TR membranes and PIMs membranes, high CO_2 affinity functional groups and high fractional free volume are preferred in designing polymers based on solution-diffusion mechanism. However, performance degradation caused by plasticization requires special attention and a more detailed investigation for industrial application scenarios. As to facilitated transport membranes, they generally exhibit a CO_2/N_2 selectivity above upper bound lines, but carrier saturation will cause a significant drop in performance, making it difficult for practical application. When it comes to non-polymeric membranes, some zeolite membranes such as SAPO-34 membrane have shown good mechanical stability and high separation performance beyond the upper bound. Considering the scale-up preparation difficulty and structure vulnerability to water vapor, it is still a long way from laboratory to industry application. MMMs are considered an effective way to approach industrial goals, but the dilemma encountered by polymers and inorganic fillers also needs to be solved in MMMs.

In 2010, Merkel gave a Robeson-type trade-off plot of CO_2/N_2 selectivity versus CO_2 permeance for membranes reported in the literature as useful for flue gas treatment [101]. Membranes with CO_2 permeance over 1000 GPU and CO_2/N_2 selectivity over 20 are expected to

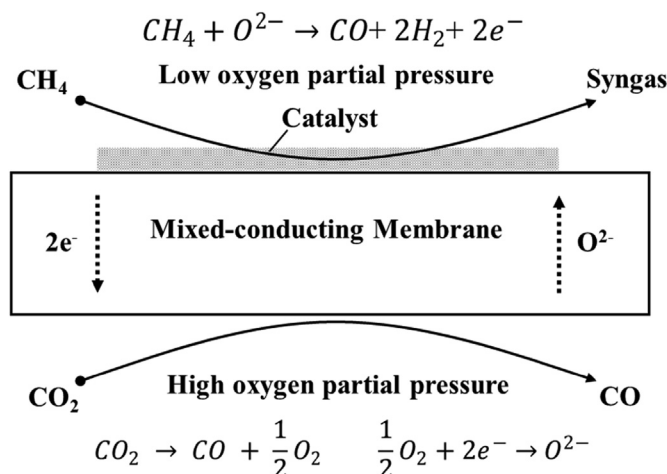$$CH_4 + O^{2-} \rightarrow CO + 2H_2 + 2e^-$$

Fig. 11. Mechanism of the membrane reaction coupling CO_2 decomposition and POM.

be economically feasible in industrial applications. Some membranes have successfully reached or surpassed this goal. In this condition, problems that may be encountered in more realistic scenarios need to be considered to further clarify the choice of materials. For example, flue gas generated from coal-fired power plants and CH_4-fired power plants are different in composition. The former contains a high concentration of CO_2 about 15% and a variety of contaminants including fly ash, SO_2 and NOx. So, electrostatic precipitator and desulfurization pretreatment process are needed and the resistance of membrane materials to sulfides also needs to be considered and evaluated. The latter contains a relatively low concentration of CO_2 ($<5\%$) which is bound to impose higher permeance demand on membrane materials. Besides, a high concentration of O_2 about 12% puts forward different requirements on the stability of membranes. In conclusion, the development of high performed membrane materials is a prerequisite for industrial application of membrane process, and the real industrialization still need more pilot plant projects and more detailed evaluation.

(2) Pre-combustion: for H_2/CO_2 separation: metallic membranes, especially Pd-based membranes, showed great attraction of high-purity H_2 production. The disadvantages of hydrogen embrittlement, performance degradation to sulfur, limited lifespan, and high membrane costs largely restricted Pb-based membranes in large-scale H_2 separation. Some new membrane materials such as GO, MOFs and MXenes have demonstrated high H_2/CO_2 separation performance, far beyond the upper bound line. However, the repeatability and industrial reliability still need to be investigated. As to polymeric membranes, glassy polymers with high FFV and mechanical stability demonstrate good H_2 permeability, but low-temperature operation requirements and poor H_2/CO_2 selectivity make them less attractive. Although PBIs exhibit relatively high H_2/CO_2 selectivity, the H_2 permeability is inferior because of polymer chain packing. Since PBI shows increased permeance at high temperatures, PBI-based membranes and mixed-matrix membranes (e.g., MMMs) can be suitable for high-temperature syngas purification. For CO_2/H_2 separation, facilitated transport membranes have shown high CO_2/H_2 selectivity at a temperature over 100°C and are not restricted by the upper bound line, which is very attractive in pre-combustion. It is worth noting that no matter what kind of membrane materials, it is necessary to consider the competitive permeability and possible adverse effects of minor components such as CO and steam.

(3) Oxy-fuel combustion (O_2/N_2): polymeric membranes, such as PSf and PI are widely used due to their excellent stability. Since the low permeability of polymeric membranes, the permeability
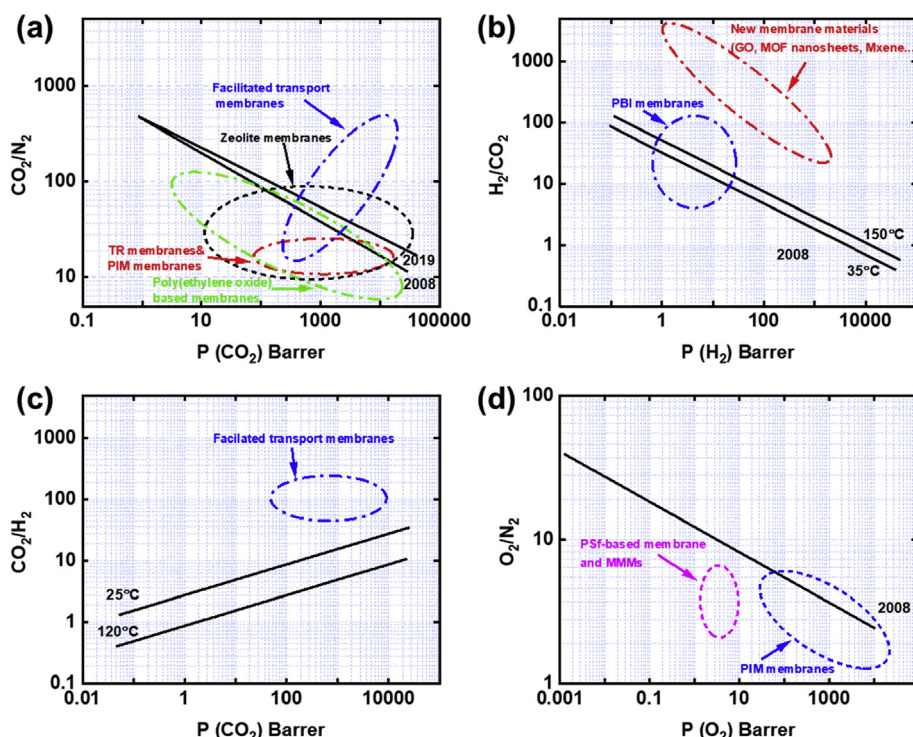
Fig. 12. Robeson plots and some performance summary [44,85,100].

increment is of primary consideration for the future development of polymers. MMMs perform well in permeability, but the selectivity improvement is quite limited, restricted by the poor selectivity performance of the polymer matrix. Most PIMs have demonstrated high permeability but are only suitable to produce low purity O_2 due to the poor selectivity. The CMS membranes derived from PI precursors exhibit attractive O_2 permeance, but their selectivities are hard to exceed 15. Mixed ionic-electronic conducting membranes represented by perovskite display high selectivity towards oxygen up to 100%. However, expensive membrane preparation costs, high operation temperature, and structure vulnerability to CO_2 have hindered the process of industrialization.

In numerous existing CO_2 capture technologies, membrane technology does not occupy a dominant position. For example, amine adsorption has been proved successful in treating industrial gas streams and is considered a leading candidate for post-combustion. However, research shows that amine adsorption is costly and energy-intensive to meet the U.S. Department of Energy target. The CO_2 separation in the IGCC plant (pre-combustion) is more accessible and cheaper due to the high CO_2 concentration and operating pressure. Although physical absorption is a promising process and some commercial product such as Selexol has been widely used, the regeneration of sorbents by temperature swing or pressure swing is energy-intensive. Besides, the increased viscosity of absorbent solvent after interaction with CO_2 is also a problem. In the short term, membrane separation is more suitable to couple with other technologies such as adsorption and adsorption and works as an auxiliary process. But from a long-term perspective, the membrane process has a significant opportunity to be an environmentally friendly, energy-saving and low-cost separation technology with the breakthrough in membrane performance and the development in membrane technologies.

In conclusion, membrane performance is an essential parameter of the membrane separation process, which is greatly affected by membrane materials, manufacturing process and operating conditions. We noticed that most of the existing studies on CO_2 capture membrane materials are

focused on improving performance and lacking sufficient attention to other vital requirements. From the perspective of industrial application, membrane materials should be evaluated under complicated and stringent separation situations in the real world. Moreover, the feasibility and competitiveness of the membrane process hinge not only on membrane performance but also on membrane cost, efficient integration, and process intensification with other facility systems, which requires deeper collaboration between power plants and membrane developers.

Finally, CO_2 utilization related to membranes is briefly summarized, and recent studies on membrane reactors for CO_2 hydrogeneration are highlighted. Although there is still a massive gap between laboratory research and industrial application. The development of new materials and the progress of material properties will bring more vitality to membrane separation. Overall, membrane technology is considered a promising technology for carbon capture and utilization, and more efforts should be made to promote the industrial application of the membrane process.

Declarations of competing interest

There are no conflicts to declare.

Acknowledgment

References

[1] Global monitoring laboratory. https://gml.noaa.gov/ccgg/trends/gl_trend.html.
[2] Global warming of 1.5 °C. https://www.ipcc.ch/sr15/.
[3] N. Norahim, P. Yaisanga, K. Faungnawakij, T. Charinpanitkul, C. Klaysom, Recent membrane developments for CO_2 separation and capture, Chem. Eng. Technol. 41 (2) (2018) 211–223, https://doi.org/10.1002/ceat.201700406.

[4] A. Al-Mamoori, A. Krishnamurthy, A.A. Rownaghi, F. Rezaei, Carbon capture and utilization update, Energy Technol. 5 (6) (2017) 834–849, https://doi.org/10.1002/ente.201600747.

[5] D.Y.C. Leung, G. Caramanna, M.M. Maroto-Valer, An overview of current status of carbon dioxide capture and storage technologies, Renew. Sustain. Energy Rev. 39 (2014) 426–443, https://doi.org/10.1016/j.rser.2014.07.093.

[6] M.E. Boot-Handford, J.C. Abanades, E.J. Anthony, M.J. Blunt, S. Brandani, N. Mac Dowell, J.R. Fernández, M.-C. Ferrari, R. Gross, J.P. Hallett, R.S. Haszeldine, P. Heptonstall, A. Lyngfelt, Z. Makuch, E. Mangano, R.T.J. Porter, M. Pourkashanian, G.T. Rochelle, N. Shah, J.G. Yao, P.S. Fennell, Carbon capture and storage update, Energy Environ. Sci. 7 (1) (2014) 130–189, https://doi.org/10.1039/c3ee42350f.

[7] Center for climate and energy solutions. https://www.c2es.org/content/carbon-capture/.

[8] W. Xing, H. Wang, N. Xu, C. Gao, Advanced membranes: the new era of membrane research, Adv. Membr. 1 (2021) 100004. http://doi:10.1016/j.advmem.2021.100004.

[9] M. Kawakami, H. Iwanaga, Y. Hara, M. Iwamoto, S. Kagawa, Gas permeabilities of cellulose nitrate/poly(ethylene glycol) blend membranes, J. Appl. Polym. Sci. 27 (7) (1982) 2387–2393, https://doi.org/10.1002/app.1982.070270708.

[10] B. Xue, X. Li, L. Gao, M. Gao, Y. Wang, L. Jiang, CO2-selective free-standing membrane by self-assembly of a UV-crosslinkable diblock copolymer, J. Mater. Chem. 22 (21) (2012) 10918–10923, https://doi.org/10.1039/c2jm31037f.

[11] H.B. Park, C.H. Jung, Y.M. Lee, A.J. Hill, S.J. Pas, S.T. Mudie, E. Van Wagner, B.D. Freeman, D.J. Cookson, Polymers with cavities tuned for fast selective transport of small molecules and ions, Science 318 (5848) (2007) 254–258, https://doi.org/10.1126/science.1146744.

[12] Z.P. Smith, D.F. Sanders, C.P. Ribeiro, R. Guo, B.D. Freeman, D.R. Paul, J.E. McGrath, S. Swinnea, Gas sorption and characterization of thermally rearranged polyimides based on 3,3′-dihydroxy-4,4′-diamino-biphenyl (HAB) and 2,2′-bis-(3,4-dicarboxyphenyl) hexafluoropropane dianhydride (6FDA), J. Membr. Sci. (2012) 558–567, https://doi.org/10.1016/j.memsci.2012.05.050, 415-416.

[13] D.F. Sanders, R. Guo, Z.P. Smith, Q. Liu, K.A. Stevens, J.E. McGrath, D.R. Paul, B.D. Freeman, Influence of polyimide precursor synthesis route and ortho-position functional group on thermally rearranged (TR) polymer properties: conversion and free volume, Polymer 55 (7) (2014) 1636–1647, https://doi.org/10.1016/j.polymer.2014.02.001.

[14] P.M. Budd, B.S. Ghanem, S. Makhseed, N.B. McKeown, K.J. Msayib, C.E. Tattershall, Polymers of intrinsic microporosity (PIMs): robust, solution-processable, organic nanoporous materials, Chem. Commun. 2 (2004) 230–231, https://doi.org/10.1039/b311764b.

[15] C.G. Bezzu, M. Carta, A. Tonkins, J.C. Jansen, P. Bernardo, F. Bazzarelli, N.B. McKeown, A spirobifluorene-based polymer of intrinsic microporosity with improved performance for gas separation, Adv. Mater. 24 (44) (2012) 5930–5933, https://doi.org/10.1002/adma.201202393.

[16] M. Carta, M. Croad, R. Malpass-Evans, J.C. Jansen, P. Bernardo, G. Clarizia, K. Friess, M. Lanc, N.B. McKeown, Triptycene induced enhancement of membrane gas selectivity for microporous Troger's base polymers, Adv. Mater. 26 (21) (2014) 3526–3531, https://doi.org/10.1002/adma.201305783.

[17] T.-J. Kim, H. Vrålstad, M. Sandru, M.-B. Hägg, Separation performance of PVAm composite membrane for CO2 capture at various pH levels, J. Membr. Sci. 428 (2013) 218–224, https://doi.org/10.1016/j.memsci.2012.10.009.

[18] Z. Qiao, Z. Wang, C. Zhang, S. Yuan, Y. Zhu, J. Wang, S. Wang, PVAm-PIP/PS composite membrane with high performance for CO2/N2 Separation, AIChE J. 59 (1) (2013) 215–228, https://doi.org/10.1002/aic.13781.

[19] Z. Qiao, S. Zhao, M. Sheng, J. Wang, S. Wang, Z. Wang, C. Zhong, M.D. Guiver, Metal-induced ordered microporous polymers for fabricating large-area gas separation membranes, Nat. Mater. 18 (2) (2019) 163–168, https://doi.org/10.1038/s41563-018-0221-3.

[20] K.K. Chen, Y. Han, Z. Zhang, W.S.W. Ho, Enhancing membrane performance for CO2 capture from flue gas with ultrahigh MW polyvinylamine, J. Membr. Sci. 628 (2021) 119215, https://doi.org/10.1016/j.memsci.2021.119215.

[21] V. Vakharia, et al., Scale-up of amine-containing thin-film composite membranes for CO2 capture from flue gas, J. Membr. Sci. 555 (2018) 379–387, https://doi.org/10.1016/j.memsci.2018.03.074.

[22] K. Kusakabe, T. Kuroda, A. Murata, S. Morooka, formation of a Y-type zeolite membrane on a porous α-alumina tube for gas separation, industrial & engineering chemistry research 36, 1997, pp. 649–655, https://doi.org/10.1021/ie960519x, 3.

[23] J.C. Poshusta, V.A. Tuan, E.A. Pape, R.D. Noble, J.L. Falconer, Separation of light gas mixtures using SAPO-34 membranes, AIChE J. 46 (4) (2000) 779–789, https://doi.org/10.1002/aic.690460412.

[24] M.P. Bernal, J. Coronas, M. Menéndez, J. Santamaría, Separation of CO2/N2 mixtures using MFI-type zeolite membranes, AIChE J. 50 (1) (2004) 127–135, https://doi.org/10.1002/aic.10012.

[25] B. Liu, C. Tang, X. Li, B. Wang, R. Zhou, High-performance SAPO-34 membranes for CO2 separations from simulated flue gas, Microporous and Mesoporous Materials, 292, 2020, p. 109712, https://doi.org/10.1016/j.micromeso.2019.109712.

[26] Z. Rui, J.B. James, A. Kasik, Y.S. Lin, Metal-organic framework membrane process for high purity CO2 production, AIChE J. 62 (11) (2016) 3836–3841, https://doi.org/10.1002/aic.15367.

[27] A. Jomekian, R.M. Behbahani, T. Mohammadi, A. Kargari, Innovative layer by layer and continuous growth methods for synthesis of ZIF-8 membrane on porous polymeric support using poly(ether-block-amide) as structure directing agent for gas separation, Microporous Mesoporous Mater. 234 (2016) 43–54, https://doi.org/10.1016/j.micromeso.2016.07.008.

[28] S. Li, C.Q. Fan, High-flux SAPO-34 membrane for CO2/N2 separation, Ind. Eng. Chem. Res. 49 (9) (2010) 4399–4404, https://doi.org/10.1021/ie902082f.

[29] E. Hayakawa, S. Himeno, Synthesis of all-silica ZSM-58 zeolite membranes for separation of CO2/CH4 and CO2/N2 gas mixtures, Microporous Mesoporous Mater. 291 (2020) 109695, https://doi.org/10.1016/j.micromeso.2019.109695.

[30] B. Wang, Y. Zheng, J. Zhang, W. Zhang, F. Zhang, W. Xing, R. Zhou, Separation of light gas mixtures using zeolite SSZ-13 membranes, Microporous Mesoporous Mater. 275 (2019) 191–199, https://doi.org/10.1016/j.micromeso.2018.08.032.

[31] B. Wang, N. Hu, H. Wang, Y. Zheng, R. Zhou, Improved AlPO-18 membranes for light gas separation, J. Mater. Chem. 3 (23) (2015) 12205–12212, https://doi.org/10.1039/c5ta01260k.

[32] M. Liu, K. Xie, M.D. Nothling, P.A. Gurr, S.S.L. Tan, Q. Fu, P.A. Webley, G.G. Qiao, Ultrathin metal-organic framework nanosheets as a gutter layer for flexible composite gas separation membranes, ACS Nano 12 (11) (2018) 11591–11599, https://doi.org/10.1021/acsnano.8b06811.

[33] H. Yin, J. Wang, Z. Xie, J. Yang, J. Bai, J. Lu, Y. Zhang, D. Yin, J.Y. Lin, A highly permeable and selective amino-functionalized MOF CAU-1 membrane for CO2/N2 separation, Chem. Commun. 50 (28) (2014) 3699–3701, https://doi.org/10.1039/c4cc00068d.

[34] M. Rungta, G.B. Wenz, C. Zhang, L. Xu, W. Qiu, J.S. Adams, W.J. Koros, Carbon molecular sieve structure development and membrane performance relationships, Carbon 115 (2017) 237–248, https://doi.org/10.1016/j.carbon.2017.01.015.

[35] R. Kumar, C. Zhang, A.K. Itta, W.J. Koros, Highly permeable carbon molecular sieve membranes for efficient CO2/N2 separation at ambient and subambient temperatures, J. Membr. Sci. 583 (2019) 9–15, https://doi.org/10.1016/j.memsci.2019.04.033.

[36] M. Hou, W. Qi, L. Li, R. Xu, J. Xue, Y. Zhang, C. Song, T. Wang, Carbon molecular sieve membrane with tunable microstructure for CO2 separation: effect of multiscale structures of polyimide precursors, J. Membr. Sci. 635 (2021) 119541, 10.1016-/j.memsci.2021.119541.

[37] F. Zhou, H.N. Tien, W.L. Xu, J.T. Chen, Q. Liu, E. Hicks, M. Fathizadeh, S. Li, M. Yu, Ultrathin graphene oxide-based hollow fiber membranes with brush-like CO2-philic agent for highly efficient CO2 capture, Nat. Commun. 8 (1) (2017) 2107, https://doi.org/10.1038/s41467-017-02318-1.

[38] T.-H. Bae, J.R. Long, CO2/N2 separations with mixed-matrix membranes containing Mg2(dobdc) nanocrystals, Energy Environ. Sci. 6 (12) (2013) 3565–3569, https://doi.org/10.1039/c3ee42394h.

[39] Q. Xin, J. Ouyang, T. Liu, Z. Li, Z. Li, Y. Liu, S. Wang, H. Wu, Z. Jiang, X. Cao, Enhanced interfacial interaction and CO2 separation performance of mixed matrix membrane by incorporating polyethylenimine-decorated metal-organic frameworks, ACS Appl. Mater. Interfaces 7 (2) (2015) 1065–1077, https://doi.org/10.1021/am504742q.

[40] J. Shen, G. Liu, K. Huang, Q. Li, K. Guan, Y. Li, W. Jin, UiO-66-polyether block amide mixed matrix membranes for CO2 separation, J. Membr. Sci. 513 (2016) 155–165, https://doi.org/10.1016/j.memsci.2016.04.045.

[41] Y. Ban, Z. Li, Y. Li, Y. Peng, H. Jiao, A. Guo, P. Wang, Q. Yang, C. Zhong, W. Yang, Confinement of ionic liquids in nanocages: tailoring the molecular sieving properties of ZIF-8 for membrane-based CO2 capture, Angew. Chem. Int. Ed. 54 (51) (2015) 15483–15487, https://doi.org/10.1002/anie.201505508.

[42] J. Shen, G. Liu, K. Huang, W. Jin, K.R. Lee, N. Xu, Membranes with fast and selective gas-transport channels of laminar graphene oxide for efficient CO2 capture, Angew. Chem. Int. Ed. 54 (2) (2015) 578–582, https://doi.org/10.1002/anie.201409563.

[43] Z. Qiao, S. Zhao, J. Wang, S. Wang, Z. Wang, M.D. Guiver, A highly permeable aligned montmorillonite mixed-matrix membrane for CO2 separation, Angew. Chem. Int. Ed. 55 (32) (2016) 9321–9325, https://doi.org/10.1002/anie.201603211.

[44] L.M. Robeson, The upper bound revisited, J. Membr. Sci. 320 (1–2) (2008) 390–400, https://doi.org/10.1016/j.memsci.2008.04.030.

[45] X. Yang, W. Zheng, Y. Xi, W. Guan, X. Yan, X. Ruan, C. Ma, Y. Dai, G. He, Constructing low-resistance and high-selectivity transport multi-channels in mixed matrix membranes for efficient CO2 separation, J. Membr. Sci. 624 (2021), https://doi.org/10.1016/j.mem-sci.2020.119046.

[46] A.A. Shamsabadi, A.P. Isfahani, S.K. Salestan, A. Rahimpour, B. Ghalei, E. Sivaniah, M. Soroush, Pushing rubbery polymer membranes to be economic for CO2 separation: embedment with Ti3C2Tx MXene nnosheets, ACS Appl. Mater. Interfaces 12 (3) (2020) 3984–3992, https://doi.org/10.1021/acsami.9b19960.

[47] V. Nafisi, M.-B. Hägg, Development of dual layer of ZIF-8/PEBAX-2533 mixed matrix membrane for CO2 capture, J. Membr. Sci. 459 (2014) 244–255, https://doi.org/10.1016/j.memsci.2014.02.002.

[48] A.F. Bushell, M.P. Attfield, C.R. Mason, P.M. Budd, Y. Yampolskii, L. Starannikova, A. Rebrov, F. Bazzarelli, P. Bernardo, J. Carolus Jansen, M. Lanč, K. Friess, V. Shantarovich, V. Gustov, V. Isaeva, Gas permeation parameters of mixed matrix membranes based on the polymer of intrinsic microporosity PIM-1 and the zeolitic imidazolate framework ZIF-8, J. Membr. Sci. 427 (2013) 48–62, https://doi.org/10.1016/j.memsci.2012.09.035.

[49] G.L. Holleck, Diffusion and solubility of hydrogen in palladium and palladium–silver alloys, J. Phys. Chem. 74 (3) (2002) 503–511, https://doi.org/10.1021/j100698a005.

[50] A.S. Augustine, I.P. Mardilovich, N.K. Kazantzis, Y. Hua Ma, Durability of PSS-supported Pd-membranes under mixed gas and water-gas shift conditions, J. Membr. Sci. (2012) 213–220, https://doi.org/10.1016/j.memsci.2012.05.001, 415-416.

[51] H.D. Tong, F.C. Gielens, J.G.E. Gardeniers, H.V. Jansen, C.J.M. van Rijn, M.C. Elwenspoek, W. Nijdam, Microfabricated palladium-silver alloy membranes and their application in hydrogen separation, Industrial & Engineering Chemistry Research 43(15), 2004, pp. 4182–4187, https://doi.org/10.1021/ie034293r.

[52] R.M. de Vos, H. Verweij, High-selectivity, high-flux silica membranes for gas separation, Science 279 (5357) (1998) 1710–1711, https://doi.org/10.1126/science.279.5357.1710.

[53] S.C. Rodrigues, M. Andrade, J. Moffat, F.D. Magalhães, A. Mendes, Preparation of carbon molecular sieve membranes from an optimized ionic liquid-regenerated cellulose precursor, J. Membr. Sci. 572 (2019) 390–400, https://doi.org/10.1016/j.memsci.2018.11.027.

[54] L. Lei, F. Pan, A. Lindbrathen, X. Zhang, M. Hillestad, Y. Nie, L. Bai, X. He, M.D. Guiver, Carbon hollow fiber membranes for a molecular sieve with precise-cutoff ultramicropores for superior hydrogen separation, Nat. Commun. 12 (1) (2021) 268, https://doi.org/10.1038/s41467-020-20628-9.

[55] X. Gu, Z. Tang, J. Dong, On-stream modification of MFI zeolite membranes for enhancing hydrogen separation at high temperature, Microporous Mesoporous Mater. 111 (1–3) (2008) 441–448, https://doi.org/10.1016/j.micromeso.2007.08.039.

[56] A. Huang, Y. Chen, N. Wang, Z. Hu, J. Jiang, J. Caro, A highly permeable and selective zeolitic imidazolate framework ZIF-95 membrane for H_2/CO_2 separation, Chem. Commun. 48 (89) (2012) 10981–10983, https://doi.org/10.1039/c2cc35691k.

[57] X. Ma, Y. Li, A. Huang, Synthesis of nano-sheets seeds for secondary growth of highly hydrogen permselective ZIF-95 membranes, J. Membr. Sci. 597 (2020) 117629, https://doi.org/10.1016/j.memsci.2019.117629.

[58] Y. Peng, Y. Li, Y. Ban, H. Jin, W. Jiao, X. Liu, W. Yang, Membranes. Metal-organic framework nanosheets as building blocks for molecular sieving membranes, Science 346 (6215) (2014) 1356–1359, https://doi.org/10.1126/science.1254227.

[59] Y. Peng, Y. Li, Y. Ban, W. Yang, Two-Dimensional metal-organic framework nanosheets for membrane-based gas separation, Angew. Chem. Int. Ed. 56 (33) (2017) 9757–9761, https://doi.org/10.1002/anie.201703959.

[60] J. Shen, G. Liu, K. Huang, Z. Chu, W. Jin, N. Xu, Subnanometer Two-Dimensional graphene oxide channels for ultrafast gas sieving, ACS Nano 10 (3) (2016) 3398–3409, https://doi.org/10.1021/acsnano.5b07304.

[61] L. Ding, Y. Wei, L. Li, T. Zhang, H. Wang, J. Xue, L.X. Ding, S. Wang, J. Caro, Y. Gogotsi, MXene molecular sieving membranes for highly efficient gas separation, Nat. Commun. 9 (1) (2018) 155, https://doi.org/10.1038/s41467-017-02529-6.

[62] H.S.M. Suhaimi, M.N.I.M. Khir, C.P. Leo, A.L. Ahmad, Preparation and characterization of polysulfone mixed-matrix membrane incorporated with palladium nanoparticles dispersed in polyvinylpyrrolidone for hydrogen separation, J. Polym. Res. 21 (2014) 428, https://doi.org/10.1007/s10965-014-0428-1.

[63] E.V. Perez, G.J.D. Kalaw, J.P. Ferraris, K.J. Balkus, I.H. Musselman, Amine-functionalized (Al) MIL-53/VTEC™ mixed-matrix membranes for H_2/CO_2 mixture separations at high pressure and high temperature, J. Membr. Sci. 530 (2017) 201–212. http://doi.org/10.1016/j.memsci.2017.02.003.

[64] X. Li, R.P. Singh, K.W. Dudeck, K.A. Berchtold, B.C. Benicewicz, Influence of polybenzimidazole main chain structure on H_2/CO_2 separation at elevated temperatures, J. Membr. Sci. 461 (2014) 59–68, https://doi.org/10.1016/j.memsci.2014.03.008.

[65] T. Yang, T.-S. Chung, High performance ZIF-8/PBI nano-composite membranes for high temperature hydrogen separation consisting of carbon monoxide and water vapor, Int. J. Hydrogen Energy 38 (1) (2013) 229–239, https://doi.org/10.1016/j.ijhydene.2012.10.045.

[66] L. Zhu, M.T. Swihart, H. Lin, Unprecedented size-sieving ability in polybenzimidazole doped with polyprotic acids for membrane H_2/CO_2 separation, Energy Environ. Sci. 11 (1) (2018) 94–100, https://doi.org/10.1039/c7ee02865b.

[67] B.W. Rowe, L.M. Robeson, B.D. Freeman, D.R. Paul, Influence of temperature on the upper bound: theoretical considerations and comparison with experimental results, J. Membr. Sci. 360 (1–2) (2010) 58–69, https://doi.org/10.1016/j.memsci.2010.04.047.

[68] Y.S. Do, J.G. Seong, S. Kim, J.G. Lee, Y.M. Lee, Thermally rearranged (TR) poly(benzoxazole-co-amide) membranes for hydrogen separation derived from 3,3′-dihydroxy-4,4′-diamino-biphenyl (HAB), 4,4′-oxydianiline (ODA) and isophthaloyl chloride (IPCl), J. Membr. Sci. 446 (2013) 294–302, https://doi.org/10.1016/j.memsci.2013.06.059.

[69] Y. Zhuang, J.G. Seong, Y.S. Do, W.H. Lee, M.J. Lee, Z. Cui, A.E. Lozano, M.D. Guiver, Y.M. Lee, Soluble, microporous, Troger's Base copolyimides with tunable membrane performance for gas separation, Chem. Commun. 52 (19) (2016) 3817–3820, https://doi.org/10.1039/c5cc09783e.

[70] Merkel, T. Mixed-gas permeation of syngas components in poly(dimethylsiloxane) and poly(1-trimethylsilyl-1-propyne) at elevated temperatures. J. Membr. Sci. 191, 85-94, http://doi.org/10.1016/s0376-7388(01)00452-00455.

[71] M. Shan, X. Liu, X. Wang, I. Yarulina, B. Seoane, F. Kapteijn, J. Gascon, Facile manufacture of porous organic framework membranes for precombustion CO_2 capture, Sci. Adv. 4 (9) (2018) 1698, https://doi.org/10.1126/sciadv.aau1698.

[72] V.I. Bondar, B.D. Freeman, I. Pinnau, Gas transport properties of poly(ether-b-amide) segmented block copolymers, J. Polym. Sci. B Polym. Phys. 38 (15) (2000) 2051–2062, http://doi.org/10.1002/1099-0488(20000801)38:15<2051::Aid-polb100>3.0.Co;2-d.

[73] J. Zou, W.S.W. Ho, CO_2-selective polymeric membranes containing amines in crosslinked poly(vinyl alcohol), J. Membr. Sci. 286 (2006) 310–321. http://doi:10.1016/j.memsci.2006.10.013.

[74] Y. Yang, Y. Han, R. Pang, W.S.W. Ho, Amine-containing membranes with functionalized multi-walled carbon nanotubes for CO_2/H_2 separation, Membranes 10 (2020) 333. http://doi:10.3390/membranes10110333.

[75] K. Ghosal, B.D. Freeman, Gas separation using polymer membranes: an overview, Polym. Adv. Technol. 5 (11) (1994) 673–697, https://doi.org/10.1002/pat.1994.220051102.

[76] D. Wang, W.K. Teo, K. Li, Preparation and characterization of high-flux polysulfone hollow fibre gas separation membranes, J. Membr. Sci. 204 (1–2) (2002), https://doi.org/10.1016/s0376-7388(02)00047-00049, 247-256.

[77] I. Pinnau, W.J. Koros, Relationship between substructure resistance and gas separation properties of defect-free integrally skinned asymmetric membranes, Industrial & Engineering Chemistry Research 30(8), 2002, pp. 1837–1840, https://doi.org/10.1021/ie00056a024.

[78] M. Niwa, H. Kawakami, S. Nagaoka, T. Kanamori, T. Shinbo, Fabrication of an asymmetric polyimide hollow fiber with a defect-free surface skin layer, J. Membr. Sci. 171 (2) (2000), https://doi.org/10.1016/s0376-7388(00)00306-00309, 253-261.

[79] P. Budd, K. Msayib, C. Tattershall, B. Ghanem, K. Reynolds, N. McKeown, D. Fritsch, Gas separation membranes from polymers of intrinsic microporosity, J. Membr. Sci. 251 (1–2) (2005) 263–269, https://doi.org/10.1016/j.memsci.2005.01.009.

[80] B. Zornoza, B. Seoane, J.M. Zamaro, C. Tellez, J. Coronas, Combination of MOFs and zeolites for mixed-matrix membranes, ChemPhysChem 12 (2011) 2781–2785. http://doi:10.1002/cphc.201100583.

[81] J. Han, L. Bai, S. Luo, B. Yang, Y. Bai, S. Zeng, X. Zhang, Ionic liquid cobalt complex as O_2 carrier in the PIM-1 membrane for O_2/N_2 separation, Separ. Purif. Technol. 248 (2020) 117041, https://doi.org/10.1016/j.seppur.2020.117041.

[82] C.W. Jones, W.J. Koros, Carbon molecular sieve gas separation membranes-I. Preparation and characterization based on polyimide precursors, Carbon 32 (8) (1994) 1419–1425, https://doi.org/10.1016/0008-6223(94)90135-x.

[83] S. Fu, G.B. Wenz, E.S. Sanders, S.S. Kulkarni, W. Qiu, C. Ma, W.J. Koros, Effects of pyrolysis conditions on gas separation properties of 6FDA/DETDA: DABA(3:2) derived carbon molecular sieve membranes, J. Membr. Sci. 520 (2016) 699–711, https://doi.org/10.1016/j.memsci.2016.08.013.

[84] Q. Liu, T. Wang, J. Qiu, Y. Cao, A novel carbon/ZSM-5 nanocomposite membrane with high performance for oxygen/nitrogen separation, Chem. Commun. 11 (2006) 1230–1232, https://doi.org/10.1039/b516519a.

[85] N.F. Himma, A.K. Wardani, N. Prasetya, P.T.P. Aryanti, I.G. Wenten, Recent progress and challenges in membrane-based O_2/N_2 separation, Rev. Chem. Eng. 35 (5) (2019) 591–625, https://doi.org/10.1515/revce-2017-0094.

[86] Y. Teraoka, H.-M. Zhang, S. Furukawa, N. Yamazoe, Oxygen Permeation through perovskite-type oxides, Chem. Lett. 14 (11) (1985) 1743–1746, https://doi.org/10.1246/cl.1985.1743.

[87] L. Yang, X. Gu, L. Tan, W. Jin, L. Zhang, N. Xu, Oxygen transport properties and stability of mixed-conducting ZrO_2-promoted $SrCo_{0.4}Fe_{0.6}O_{3-\delta}$ oxides, Ind. Eng. Chem. Res. 41 (17) (2002) 4273–4280, https://doi.org/10.1021/ie020132w.

[88] X. Zhu, H. Wang, W. Yang, Novel cobalt-free oxygen permeable membrane, Chem. Commun. 9 (2004) 1130–1131, https://doi.org/10.1039/b400857j.

[89] J. Zhu, G. Liu, Z. Liu, Z. Chu, W. Jin, N. Xu, Unprecedented perovskite oxyfluoride membranes with high-efficiency oxygen ion transport paths for low-temperature oxygen permeation, Adv. Mater. 28 (18) (2016) 3511–3515, https://doi.org/10.1002/adma.201505959.

[90] W. Jin, Preparation of an asymmetric perovskite-type membrane and its oxygen permeability, J. Membr. Sci. 185 (2) (2001) 237–243, https://doi.org/10.1016/s03767388-(00)00650-5.

[91] J. Zhu, G. Zhang, G. Liu, Z. Liu, W. Jin, N. Xu, Perovskite hollow fibers with precisely controlled cation stoichiometry via one-step thermal processing, Adv. Mater. 29 (18) (2017) 1606377, https://doi.org/10.1002/adma.201606377.

[92] J. Zhu, Z. Dong, Z. Liu, K. Zhang, G. Zhang, W. Jin, Multichannel mixed-conducting hollow fiber membranes for oxygen separation, AIChE J. 60 (6) (2014) 1969–1976, https://doi.org/10.1002/aic.14471.

[93] T. Wang, Z. Liu, X. Xu, J. Zhu, G. Zhang, W. Jin, Insights into the design of nineteen-channel perovskite hollow fiber membrane and its oxygen transport behaviour, J. Membr. Sci. 595 (2020) 117600, https://doi.org/10.1016/j.memsci.2019.117600.

[94] T. Chen, Z. Wang, L. Liu, S. Pati, M.H. Wai, S. Kawi, Coupling CO_2 separation with catalytic reverse water-gas shift reaction via ceramic-carbonate dual-phase membrane reactor, Chem. Eng. J. 379 (2020) 122182, https://doi.org/10.1016/j.cej.2019.122182.

[95] H. Li, C. Qiu, S. Ren, Q. Dong, S. Zhang, F. Zhou, X. Liang, J. Wang, S. Li, M. Yu, Na^+-gated water-conducting nanochannels for boosting CO_2 conversion to liquid fuels, Science 367 (6478) (2020) 667–671, https://doi.org/10.1126/science.aaz6053.

[96] W. Yue, Y. Li, W. Wei, J. Jiang, J. Caro, A. Huang, Highly Selective CO_2 Conversion to methanol in a bifunctional zeolite catalytic membrane reactor, Angew. Chem. Int. Ed. 60 (33) (2021) 18289–18294, https://doi.org/10.1002/anie.202106277.

[97] W. Jin, C. Zhang, P. Zhang, Y. Fan, N. Xu, Thermal decomposition of carbon dioxide coupled with POM in a membrane reactor, AIChE J. 52 (7) (2006) 2545–2550, https://doi.org/10.1002/aic.10850.

[98] C. Zhang, X. Chang, Y. Fan, W. Jin, N. Xu, Improving performance of a dense membrane reactor for thermal decomposition of CO_2 via surface modification, Ind. Eng. Chem. Res. 46 (7) (2007) 2000–2005, https://doi.org/10.1021/ie060913n.

[99] K. Zhang, G. Zhang, Z. Liu, J. Zhu, N. Zhu, W. Jin, Enhanced stability of membrane reactor for thermal decomposition of CO_2 via porous-dense-porous triple-layer

composite membrane, J. Membr. Sci. 471 (2014) 9–15, https://doi.org/10.1016/j.memsci.2014.06.060.

[100] Y. Han, W.S.W. Ho, Polymeric membranes for CO_2 separation and capture, J. Membr. Sci. 628 (2021) 119244. http://doi:10.1016/j.memsci.2021.119244.

[101] T.C. Merkel, H. Lin, X. Wei, R. Baker, Power plant post-combustion carbon dioxide capture: an opportunity for membranes, J. Membr. Sci. 359 (2010) 126–139, https://doi.org/10.1016/j.memsci.2009.10.041.

Guining Chen received her bachelor degree in chemical engineering and technology from Nanjing Tech University in 2017. She then joined Prof. Wanqin Jin's research group in the same year in Nanjing Tech University. She is now a Ph.D. candidate in the Department of Chemical engineering. Her research is focused on the metal-organic framework membranes for gas separation.

Dr. Wanqin Jin is a professor of Chemical Engineering at Nanjing Tech University, the Deputy-director of the State Key laboratory of Materials-oriented Chemical Engineering, and the Chief-scientist of the National Basic Research Program of China (973 Program). He received his Ph.D. from the Nanjing University of Technology in 1999. He was a research associate at the Institute of Materials Research & Engineering of Singapore (2001), an Alexander von Humboldt Research Fellow (2001–2013), visiting professors at Arizona State University (2007) and Hiroshima University (2011, JSPS invitation fellowship). His current research focuses on the development of membrane materials, membrane processes, and membrane reactors. He has published over 300 SCI-tracked journal publications in Nature, Nat. Rev. Mater., Chem. Soc. Rev., Nat. Commun., Adv. Mater., Adv. Funct. Mater., Angew. Chem. Int. Ed, J. Am. Chem. Soc., AIChE J., J. Membr. Sci., Chem. Eng. Sci. et al., with over 21,000 SCI citations (H-index 76), wrote two monographs, contributed 10+ book chapters and held 40+ authorized patents. He presented over 60 plenary, keynote lectures, and invited speeches in international conferences and was co-chair of the 10th International Congress on Membrane and membrane Processes (ICOM2014). He is now an editor of the Journal of Membrane Science and on the Editorial Boards of Chinese Journal of Chemical Engineering, Asia-Pacific Journal of Chemical Engineering, and Inorganic Materials. He is a fellow of the royal society of chemistry and a council member of Aseanian Membrane Society (AMS). In 2019, the Institution of Chemical Engineers awarded "The Underwood Medal" to him for his significant, sustained contribution to research in the area of separations.